CHAPTER VI
DIRECT METHYLATION OF BENZENE WITH METHANE OVER Mo/HZSM-5 CATALYST

6.1 Abstract

Although Mo/HZSM-5 catalyst cannot induce xylenes formation, it is at least able to catalyze the methylation reaction, the desired reaction route, as a result of toluene formation. However, this reaction is predominantly competed by benzene coupling reaction, in which naphthalene is obtained. Mo/HZSM-5 activated under reductive conditions showed highest activity compared to other activating conditions. Metallic Mo dominated in Mo/HZSM-5 catalyst following this activation and it was thus suggested to be an active site for the reaction, nonetheless metallic Mo is susceptible to the reaction conditions as it tends to be oxidized under reaction atmosphere evidenced by the XPS results. Applying H_2 co-feed significantly effects on product selectivity, which naphthalene formation is impeded and toluene become a major product, but does not improve Mo stability. Study on the effect of Mo loading confirmed a role of Mo species in activating the reaction, of which benzene conversion increases with Mo loading, while product selectivity seems to rely on catalyst acidity. Increasing reaction temperature increases benzene conversion but lower toluene formation with higher heavy aromatic formation. Moreover, reaction parameters (e.g., methane to benzene feed molar ratio and WHSV) have an influence to catalyst activity and selectivity.

Keywords: Methylation, Benzene, Methane, Mo/HZSM-5, Metallic Mo

6.2 Introduction

The conversion of benzene into higher value aromatics has been an interesting topic to many scientists and engineers. Methylation of benzene by utilizing methane as an alkylating agent is interesting and challenging. The major benefit of this approach is the utilization of abundant and low cost methane. Methylated products, such as toluene, xylenes and heavier aromatics, can be expected from this reaction. Since the reaction is not thermodynamically favorable due to the high stability of methane, the catalytic activation with a very active catalyst is required. The conversion of benzene by reaction with methane was first observed using zeolites based catalysts such as H-Y, H-beta and HZSM-5 (Kennedy et al., 1994) under severe conditions (i.e., high pressure and temperature). Their results suggested that all reaction products are solely derived from benzene, possibly through catalytic cracking and alkylation. Later, the metal loaded zeolites such as copper, cobalt (Adebajo et al., 2000) or platinum (Lukyanov et al., 2009) were demonstrated as they provided better activity than pure zeolites with Brönsted protons; however, conversion and selectivity on these catalysts were still not of practical use.

Because of the high stability of methane, the activation of methane into more active species is primarily considered. A carbocation CH_3^+ species (electrophile) seems to be the most theoretically appropriate for this attempt because benzene is naturally a nucleophile, a chemical species that is able to donate electron pairs to an electrophile to form a chemical bond (Mcketta, 1993). Accordingly, electrophilic substitution on a benzene ring is a preferred methylation reaction route. Mo/HZSM-5 was widely accepted as a promising catalyst for the methane aromatization reaction (Liu et al., 2001; Liu et al., 2006; Solymosi et al., 1995; Solymosi et al., 1996; Szöke et al., 1996; Wang et al., 1997; Weckhuysen et al., 1998). Although a wide variety of activated methane species can be generated over this catalyst, there is a possibility that carbenium ions (CH_3^+) formed and reacted with benzene (if existed/added) to form some methylated products. For Mo/HZSM-5 catalyst for methane aromatization, Mo carbide species were proposed to be active sites in this catalyst. To obtain Mo carbide species, Mo/HZSM-5 catalyst was

generally treated by methane at high temperature (Bouchy et al., 2000; Liu, et al., 2006; Solymosi et al., 1996). Moreover, different treatment procedures lead to different types of Mo carbides. Stable β-Mo_2C species in hexagonally close-packed (hcp) structures can be obtained by heating MoO_3 species in a methane flow from room temperature to 710 °C, while metastable α-MoC_{1-x} species in face-centered cubic (fcc) structures can be attained by reducing MoO_3 species in H_2 and, subsequently, carburizing in CH_4 (Bouchy et al., 2000; Derouane-Abd Hamid et al., 2000; Liu et al., 2006). In addition to Mo carbide species generated after the carburization step, Mo oxycarbide (MoO_xC_y) is another Mo species simultaneously generated from partial carburization of MoO_x species associating with the Brönsted acid sites in Mo/HZSM-5 (Liu et al., 2006; Ma et al., 2000). Different Mo species or even different structures exhibit different activity and selectivity for the reaction. For instance, a α-MoC_{1-x} species in the fcc form was proposed to be more active than β-Mo_2C species in the hcp form for the methane aromatization reaction (Liu et al., 2006). Mo oxycarbide (MoO_xC_y) also exhibits its activity for this reaction (Liu et al., 2006; Ma et al., 2000).

Due to a satisfactory activity of Mo/HZSM-5 in activating methane, in this work Mo/HZSM-5 catalyst was selected to study its ability to catalyze the methylation reaction of benzene with methane. Three different activation conditions (e.g., carburization, reduction, and oxidation) were applied for the Mo/HZSM-5 catalyst. This was done to explore the most suitable activating condition as well as to develop deep insight into which Mo species is the most appropriate one. The catalyst was mainly characterized using XPS. Effects of Mo loading, H_2 co-feed, and reaction conditions (e.g., reaction temperature, methane to benzene feed molar ration, and WHSV) on benzene conversion and product selectivity were also demonstrated.

6.3 Experimental

6.3.1 Catalyst Preparation

The catalyst support HZSM-5 (Si/Al = 22) was purchased from Tosoh. Mo/HZSM-5 was prepared by incipient wetness impregnation technique using ammonia heptamolybdate ($(NH_4)_6[Mo_7O_{24}] \cdot 4H_2O$), purchased from Carlo

Erba reagent, as a Mo precursor. The catalyst was dried at room temperature for 12 h and at 120 °C for 2 h respectively. Finally, it was calcined in a muffle furnace at 500 °C for 6 h (Liu et al., 2006). Prior to testing the reaction, catalysts were pretreated under 3 separate and different conditions including reduction (550 °C, H_2 flow, 30 min), oxidation (550 °C, O_2 flow, 30 min), and carburization (700 °C, 10%N_2/CH_4 flow, 30 min), which will be designated by the prefix of "red-", "oxi-", and "car-", respectively.

6.3.2 Catalyst Characterization

The XPS measurements; Kratos Axis Ultra^{DLD}, were performed at a base pressure of 10^{-8} Torr using Al K_a primary radiation (15 kV, 10 mA) as the X-ray source and the pass energy was set at 40 eV. The samples, which were pretreated by oxidation and carburization, were tested in a catalytic reactor and subsequently transferred to the sample holder of the XPS system for analysis. The reduced sample was tested in-situ in the catalyst reaction chamber with the Kalrez® door equipped within this XPS system. The reduction pretreatment was carried out at 550 °C under flow of 5%H_2/N_2 for 30 min. Following the reduction step, the sample was then transferred to an inlet chamber, which was subsequently evacuated until the pressure was below 5×10^{-7} Torr. Then, it was introduced into the UHV analysis chamber using a transferring probe without exposure to air. Besides the pretreated samples, all the spent samples were also tested by XPS measurements in order to compare with fresh/pretreated samples. Due to other types of carbon on catalyst samples obtained from either carburization or under reaction conditions, all binding energies were referenced to the zeolitic Si 2p peak at 102.8 eV (Weckhuysen et al., 1998). Moreover, carbon species on the catalyst samples were also distinguished.

X-ray diffractometer system; A Rigaku RINT-2200 instrument using Cu K_α radiation (1.5406 Å), and a nickel filter, was used to scan the pretreated Mo/HZSM-5 catalyst in order to investigate Mo species present after different pretreatments. The generator voltage and current were set at 40 kV and 30 mA, respectively. A scan speed of 5° (2θ)/min with a scan step of 0.02 (2θ) was used for scanning in the range of 10 to 90° (2θ). All pretreatments were performed ex-situ in a

catalytic reactor and, subsequently, transferred to a XRD sample cell. To avoid reoxidation of metallic Mo in the reduced sample as much as possible, the catalyst sample was immediately brought to scan XRD after the reduction step. Samples are required to be in powder form and held in a sample glass holder. The signal was recorded online during scanning. The Scherrer equation below was used to determine the average crystallite diameter of the particle.

$$D_h = \frac{K \cdot \lambda}{B_d \cdot \cos\theta}$$

where:

D_h = The mean size of crystalline (Å)

K = A dimensionless shape factor, 0.9

λ = X-Ray wavelength (Å)

B_d = The line broadening at half the maximum intensity $\Delta(2\theta)$ (radian)

θ = Bragg angle of the reflection (degree)

Temperature-programmed reduction (TPR); A ThermoFinnigan TPDRO 1100 instrument using a TCD detector, was used for determining the reducibility of the catalyst and verifying Mo oxides species in the catalyst. The catalyst sample was first pretreated at 120 °C under flow of 30 ml/min N_2 for 1 h to remove humidity. Then, the pretreated sample was transferred to the TPR analysis line without exposure to air. An analysis was started with a ramp rate of 10 °C/min from 50 °C to 900 °C under flow of 4.95% H_2 in N_2 (30 ml/min) and the TCD signal was recorded online.

Temperature-programmed desorption of ammonia (TPD-NH_3); A ThermoFinnigan TPDRO 1100 instrument using a TCD detector, was used to measure both acid strength and number of site of the Mo/HZSM-5 catalyst with varying Mo loadings. The catalyst sample was packed in a sample tube and pretreated at 350 °C under flow of 30 ml/min N_2 for 3 h to remove any impurities on the catalyst surface. Then, it was cooled down to 50 °C under flow of 30 ml/min N_2.

To get NH_3 adsorbed on the acidic sites of catalyst, a flow of 10% NH_3 in N_2 (20 ml/min) was introduced to a sample tube containing the treated catalyst sample for 1 h at the same temperature. After that, a flow of 30 ml/min N_2 was passed through the sample tube for 1 h in order to remove excess NH_3 left on the catalyst surface. For TPD analysis, it was heated with a ramp rate of 10 °C/min under flow of 30 ml/min N_2 and desorbed NH_3 was detected by using a TCD detector. The thermogram was recorded from 50 °C to 900 °C.

6.3.3 Catalyst Activity Test

The reaction between benzene and methane was implemented in a fixed-bed flow reactor, made of quartz (8.4 mm inside diameter and 40 cm length), at atmospheric pressure. Catalysts were packed into a quartz tube reactor at the middle of the reactor with bounding at each side (top and bottom) by quartz wool. A quartz tube was inserted and used to support the catalyst bed and also help to reduce reactor volume, thus increasing the product flow. Prior to the catalytic measurements, the packed catalyst was heated (10°C/min) to 120°C under N_2 flow (30 ml/min) and held for 30 min in order to remove humidity. Then, it was pretreated under the following conditions; reduction, oxidation, or carburization. The reactant feed stream was prepared by feeding benzene into a vaporizer. Saturated benzene at 40 °C was then carried by N_2 into a mixer, where the gas mixture of benzene, methane, and nitrogen was obtained. The feed stream was also analyzed for composition via a by-pass line before sending to the reactor. The reaction products were analyzed online by GC (Agilent 7820A), equipped with an Innowax capillary column and a flame ionization detector (FID), and a Porapack packed column combined with valve configuration and a thermal conductivity detector (TCD).

6.4 Result and Discussion

6.4.1 Catalyst Characterization

XPS spectra at Mo3d region of Mo/HZSM-5 treated with different conditions are illustrated in Figure 6.1. Typically, there are two prominent peaks in the Mo3d region, which are the $Mo3d_{5/2}$ and $Mo3d_{3/2}$ peaks occuring at lower and

higher binding energies, respectively. These binding energy peaks can be varied depending on the oxidation state of Mo species. For example, The $Mo3d_{5/2}$ and $Mo3d_{3/2}$ binding energies were 233.1 and 236.3 eV for Mo^{6+}, 231.4 and 234.6 eV for Mo^{5+}, 229.8 and 232.5 eV for Mo^{4+}, 227.6 and 230.8 eV for Mo^{0} (Solymosi et al., 1995; Wang et al., 1997). Considering freshly calcined Mo/HZSM-5, it is possible that the catalyst contains a mixture of Mo^{6+} and Mo^{5+}, as a $Mo3d_{5/2}$ peak is in between the peaks of Mo^{6+} and Mo^{5+} species. For reduced Mo/HZSM-5 represented by spectrum (b) in Figure 6.1, it is clear that Mo is completely in the metallic form as the $Mo3d_{5/2}$ peak is shifted to lower binding energy at around 227.9 eV, which is close to that of Mo^{0} species at a B.E. of 227.6 eV. Oxidation of Mo/HZSM-5 leads to the oxidation of Mo into more Mo^{6+}, which is probably in the MoO_3 form, as the $Mo3d_{5/2}$ peak on a spectrum (c) of oxidized sample more resembles the reference Mo^{6+} peak at around 233.1 eV. Following carburization pretreatment, it is more likely that some of Mo species in Mo/HZSM-5 were transformed into the Mo carbide form (Mo_2C), as evidenced by the appearance of the $Mo3d_{5/2}$ peak at around 227.9 eV. In fact, metallic Mo and the Mo in Mo_2C cannot be readily distinguished by XPS spectra in the Mo3d region because of the similarity in Mo3d binding energies of these two species. Hence, it is necessary to scan at the C1s region, if Mo_2C is formed (Chen, 1995; deVries et al., 1983; Wang et al., 1997; Wang et al., 1991). It has been explored that three carbon species can be distinguished by C1s binding energy: carbidic carbon (283.3 eV), polymeric carbon (284.5 eV), and amorphous or graphitic carbon (285.0 eV) (Leclercq et al., 1989; Ledoux et al., 1992). Furthermore, the C1s binding energy of Mo_2C species was reported at 283.85 eV by Lee and co-workers (Lee et al., 1987) and at 283.8 eV by Solymosi and co-workers (Solymosi et al., 1997). The XPS spectrum in the C1s region of carburized Mo/HZSM-5 is depicted in Figure 6.2. The obvious peak at 283.9 eV is likely attributed to carbidic carbon in the Mo_2C form. Together with the Mo3d spectrum, it can be concluded that Mo_2C was generated in Mo/HZSM-5 after carburization. However, most of the Mo still remained in the oxidized forms (i.e., Mo^{6+} and Mo^{5+}), as those peaks existed. It is noted that, at those carburization conditions, 100% of Mo_2C formation cannot be achieved. This might be due to insufficient holding time; however, it is enough to bring it to test for the reaction as Mo_2C co-existed with other species

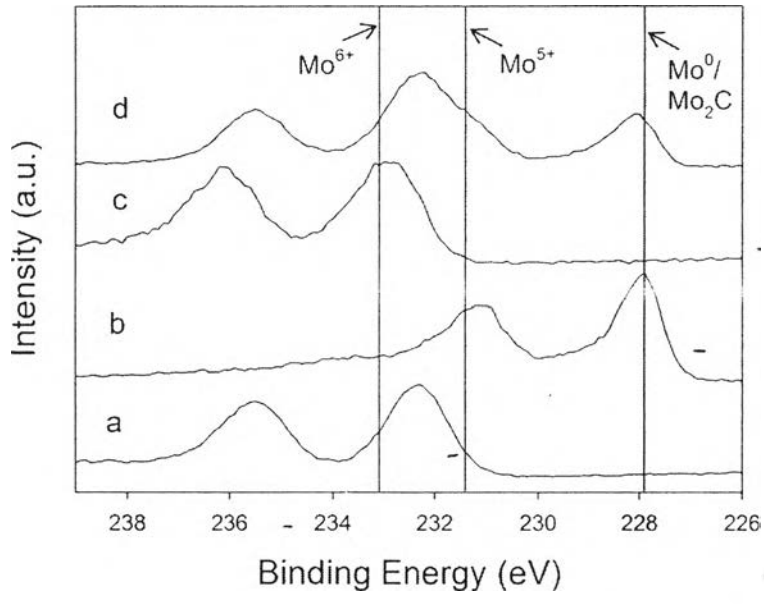

Figure 6.1 XPS spectra of Mo/HZSM-5 catalysts at Mo3d region, including (a) freshly calcined Mo/HZSM-5, (b) red-Mo/HZSM-5 (after reduction in $5\%H_2/N_2$ at 550 °C for 0.5 h), (c) oxi-Mo/HZSM-5 (after oxidation in O_2 at 550 °C for 0.5 h), (d) car-Mo/HZSM-5 (after carburization in $10\%N_2/CH_4$ at 700 °C for 0.5 h).

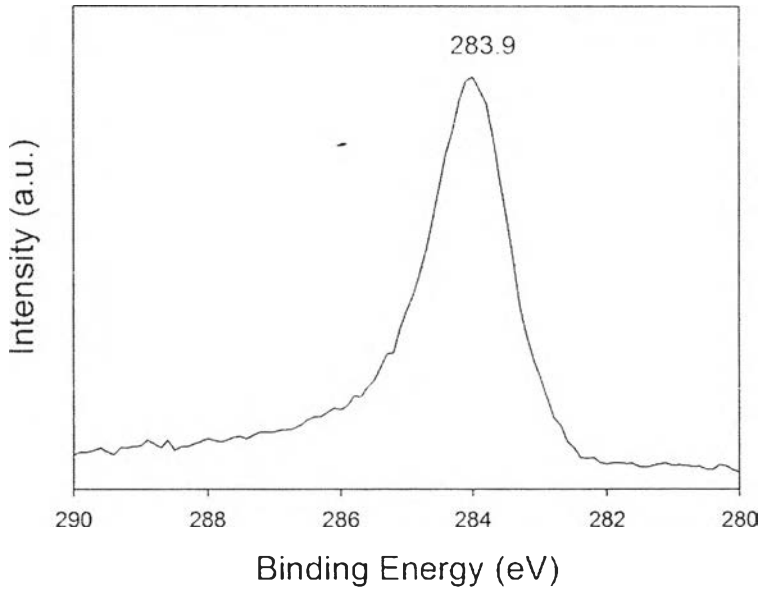

Figure 6.2 XPS spectrum at C1s region of car-Mo/HZSM-5 catalyst (after carburization in $10\%N_2/CH_4$ at 700 °C for 0.5 h).

Figure 6.3 shows the H_2-TPR profile of freshly calcined and pre-reduced Mo/HZSM-5 catalysts. Two peaks appear in the profile at ~475 °C and ~640 °C, respectively. The first peak at lower temperature is widely accepted to be the reduction of polymolybdate MoO_3 to MoO_2, while the second peak is attributed to the reduction of crystalline MoO_3 to MoO_2 (Barath et al., 1999; Jiang et al., 1999; Liu et al., 2001; Liu et al., 2006; Williams et al., 1991). Moreover, another reduction peak appearing at very high temperature (>900 °C) represents the further reduction of MoO_2 to Mo^0 (Barath et al., 1999; Jiang et al., 1999; Liu et al., 2001; Ma et al., 2000; Regalbuto et al., 1994), but it was not detected in this work due to a limitation of the instrument. However, this result at least confirms a predominant existence of MoO_3 at the initial state (after calcination), which is in agreement with the XPS results above. Pre-reduction of this catalyst was performed at 2 different temperatures (i.e., 350 °C and 550 °C) in order to evaluate the reducibility of this catalyst. It was found that, after reduction at 350 °C for 30 min, polymolybdate MoO_3 is completely reduced to MoO_2, whereas crystalline MoO_3 remains unreduced, as observed by the appearance of the second peak. Following pre-reduction at 550 C for 30 min, both polymolybdate MoO_3 and crystalline MoO_3 were successfully reduced, possibly to MoO_2. Likewise, with this condition, there was a possibility that Mo existing on the catalyst outer surface is reduced into the metallic Mo form, as described by the XPS results previously.

The XRD technique was used to investigate the species of Mo presenting in Mo/HZSM-5 catalyst before and after pretreatment with different atmospheres and the results are portrayed in Figure 6.4. It is observed that catalysts obtained after calcination and pretreatment steps can still maintain the structure of the HZSM-5 support. This shape selective structure will be beneficial to p-xylene selectivity, if xylenes are generated inside ZSM-5 pores. As expected, MoO_3 dominates in the freshly calcined Mo/HZSM-5 catalyst, indicated by the diffraction peaks of MoO_3 in HZSM-5 at $2\theta = 27.3°$ and 33.6° (Bohne et al., 2005; Bouchy et al., 2000) on a spectrum (a). By the Scherrer equation, the average crystallite size of MoO_3 is around 5.94 Å diameter. After reduction, a peak emerged at $2\theta = 40.5°$ as shown in a spectrum (b). This peak is ascribed to metallic Mo (110) (Bohne et al., 2005) with an average crystallite size of 3.05 Å.

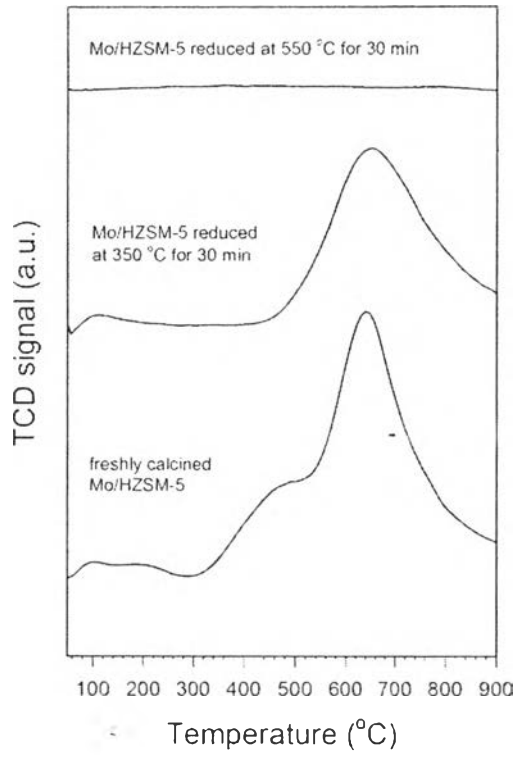

Figure 6.3 H_2-TPR profiles of freshly calcined Mo/HZSM-5 (solid line) and Mo/HZSM-5 reduced. moving up, at 350 °C for 30 min and at 550 °C for 30 min, respectively.

Although metallic Mo was generated by this reductive condition, some MoO_3 still existed as its diffraction peaks (2θ = 27.3° and 33.6°) appeared. Due to an experimental procedure (ex-situ treatment), it is likely that some metallic Mo underwent oxidation by air during transfer of the sample to the XRD instrument. However, it is enough to observe that, by this reduction condition, MoO_3 reduced into the metallic Mo form, as described by a decrease in MoO_3 peak intensities with an increase in metallic Mo peak intensity. For oxi-Mo/HZSM-5, it is obvious that MoO_3 peaks are more intense (in spectrum (c)) and, correspondingly, its average crystallite size is slightly increased to 6.53 Å compared with 5.94 Å MoO_3 in the freshly calcined catalyst. This might be due to further oxidation of Mo^{5+} to Mo^{6+} (MoO_3) as previously discussed (XPS results), thus leading to more and larger sized MoO_3 species in the catalyst. Spectrum (d) reflects the XRD pattern of car-Mo/HZSM-5. Although Mo_2C was expected to be observed according to XPS

results, XRD doesn't show any peaks of molybdenum carbides. The small fraction and tiny size of molybdenum carbide may be the reason. Nonetheless, a decrease in peak intensity of MoO_3 species suggested the transformation of this species into other forms, presumably to tiny Mo_2C species.

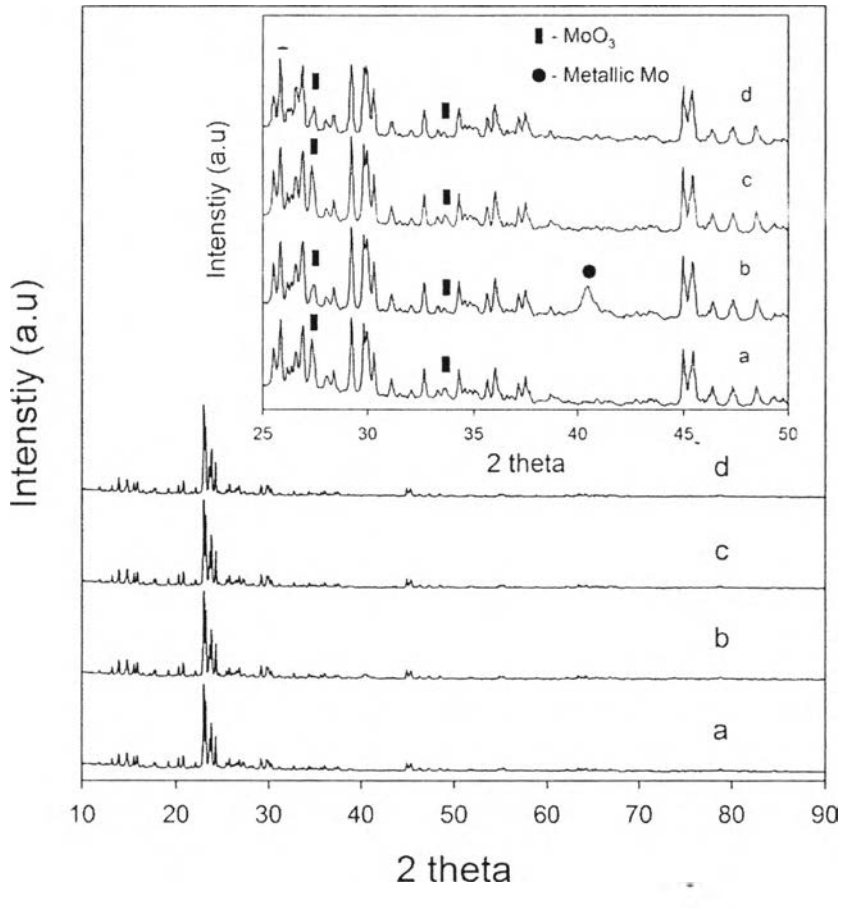

Figure 6.4 X-ray diffraction patterns, including (a) freshly calcined Mo/HZSM-5, (b) red-Mo/HZSM-5 (after reduction in $5\%H_2/N_2$ at 550 °C for 0.5 h), (c) oxi-Mo/HZSM-5 (after oxidation in O_2 at 550 °C for 0.5 h). (d) car-Mo/HZSM-5 (after carburization in $10\%N_2/CH_4$ at 700 °C for 0.5 h). HZSM-5 peaks are not indexed.

6.4.2 Catalyst Activity Test

The results of reaction tests are depicted in Figure 6.5, including benzene conversion in Figure 6.5(A), toluene selectivity in Figure 6.5(B), and heavier aromatics selectivity in Figure 6.5(C). Although toluene is not an attractive

product like xylenes, the formation of it from the reaction between benzene and methane can imply the occurrence of a methylation reaction route, a desired reaction pathway. In fact, the formation of toluene is more thermodynamically favorable than the formation of xylenes as discussed in Chapter III. If it is indeed the case that production of toluene from benzene and methane can be achieved with a satisfactory yield, it may be beneficial to convert the toluene produced to xylenes in an existing technology, Tatoray via toluene disproportionation. Therefore, as no xylene formations, the formation of toluene was explored in this part of the study.

It was found that different pretreatment conditions make the Mo/HZSM-5 catalyst exhibit differences in activity. Red-Mo/HZSM-5 showed the highest activity for benzene conversion compared to the others, but the reaction was mainly towards heavy aromatics formation as shown in Figure 6.5. Recalling the catalyst characterization results in the previous part, metallic Mo likely plays an important role in this high activity. Obviously, catalyst activity decreases with time on stream, suggesting some changes in the Mo form during the reaction (to be discussed later). On oxi-Mo/HZSM-5 catalyst, the activity was quite different from red-Mo/HZSM-5 in both activity for benzene conversion and product selectivity. Interestingly, changes in benzene conversion and product selectivity with time on stream suggest transformations of Mo species during the reaction. MoO_3 species, dominating in oxi-Mo/HZSM-5, are more likely to be transformed into metallic Mo at ~90 min of TOS as its activity for benzene conversion increased and changes in product selectivity occurred; moreover, metallic Mo formed may be subject to changes into other forms as a decrease in activity was observed. In addition, a transformation of MoO_3 into Mo_2C species is also possible along with the reaction according to the reaction conditions. It has been reported that MoO_3 can be directly carburized by methane into the hcp structures of β-Mo_2C and MoO_xC_y species (Bouchy et al., 2000; Derouane-Abd Hamid et al., 2000; Liu et al., 2006). Car-Mo/HZSM-5 did catalyze the reaction with ~2% benzene conversion but the reaction on this catalyst contributed to heavy aromatic compounds formation more than toluene formation. Naphthalene dominated in heavy aromatics with >85 wt%, suggesting benzene coupling as major reaction, while methylation the reaction of benzene into toluene was minor. Toluene formation is probably derived from the

reaction between the benzene molecule and methyl species (CH_3), generated by Mo_2C species, on Brönsted acid sites (Barthos et al., 2007). Methylation of benzene by methyl species through an electrophilic substitution mechanism was suggested. It is known that highly dispersed Mo_2C species on the external surface of the HZSM-5 zeolite are the active sites and are responsible for initial methane activation (Liu et al., 2001; Solymosi et al., 1995; Solymosi et al., 1996; Szöke et al., 1996; Wang et al., 1997; Weckhuysen et al., 1998). In addition to Mo_2C, Mo oxycarbide (MoO_xC_y), which is generated from partial carburization of MoO_x species associated with the Brönsted acid sites by methane, is also accepted as an active species for methane activation (Ma et al., 2000), but its activity is lower relative to bulk the Mo carbide forms. Furthermore, different structures of Mo carbides provide different activity. The α-MoC_{1-x} and MoO_xC_y species in face-centered cubic (fcc) structure was proposed to be more active than β-Mo_2C and MoO_xC_y species in the hexagonal close-packed (hcp) structure for the reaction of methane dehydroaromatization (MDA) (Liu et al., 2006). Metastable α-MoC_{1-x} species in the face-centered cubic (fcc) structure can be obtained from MoO_3 species by performing reduction in H_2 followed by carburization in CH_4 (Bouchy et al., 2000; Derouane-Abd Hamid et al., 2000; Liu et al., 2006). In addition, the MoO_xC_y species with an fcc structure could be simultaneously generated in Mo/HZSM-5 (Chen et al., 1995; Liu et al., 2006; Weckhuysen et al., 1998; Zhang et al., 1998). Formation of stable β-Mo_2C species in the hexagonally close-packed (hcp) structure can be obtained by carburization of MoO_3 species in a methane flow from room temperature to 710 °C (Bouchy et al., 2000; Derouane-Abd Hamid et al., 2000). During carburization of Mo supported HZSM-5, MoO_xC_y species in the hcp structure will be simultaneously generated with hcp β-Mo_2C species and the proportion of these species depends on the acidity of HZSM-5 (Liu et al., 2006). These proposed active species may exist in car-Mo/HZSM-5 and play a role in the reaction. However, likely due to their tiny sizes, they cannot be distinguished by XRD.

A

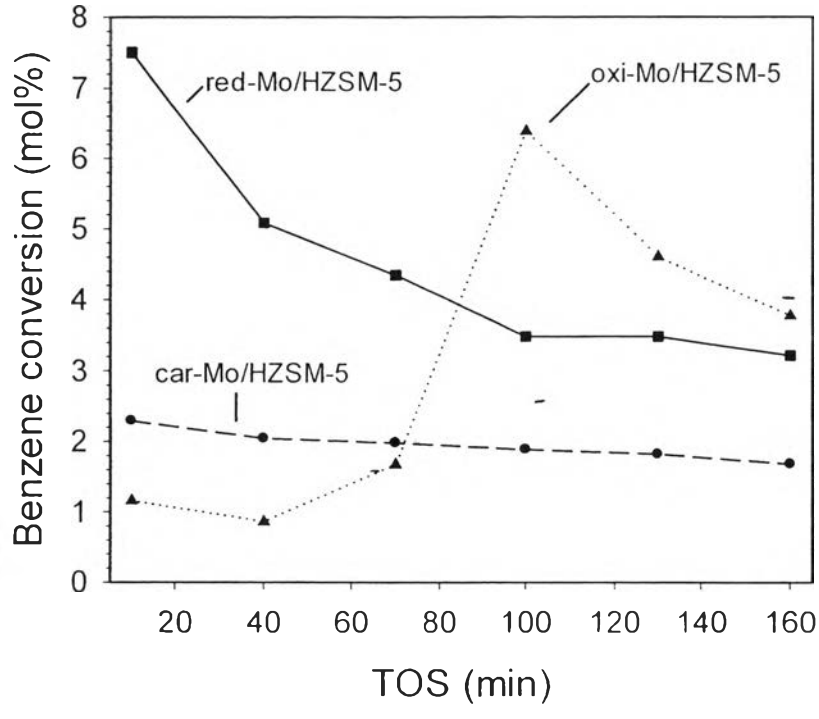
Benzene conversion (mol%)
TOS (min)
red-Mo/HZSM-5
oxi-Mo/HZSM-5
car-Mo/HZSM-5
0
1
2
3
4
5
6
7
8
20
40
60
80
100
120
140
160

B

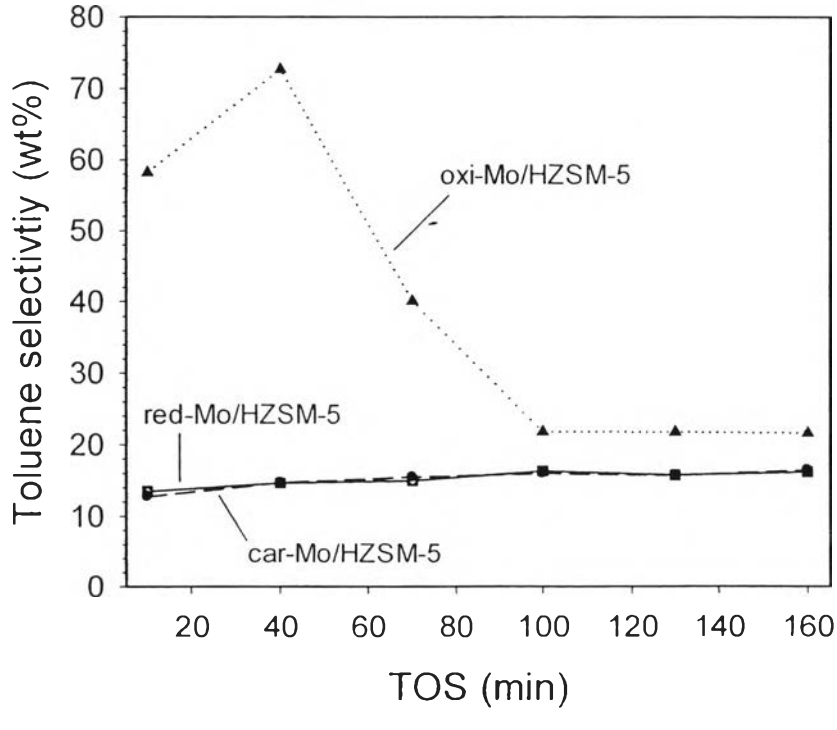
Toluene selectivtiy (wt%)
TOS (min)
oxi-Mo/HZSM-5
red-Mo/HZSM-5
car-Mo/HZSM-5
0
10
20
30
40
50
60
70
80
20
40
60
80
100
120
140
160

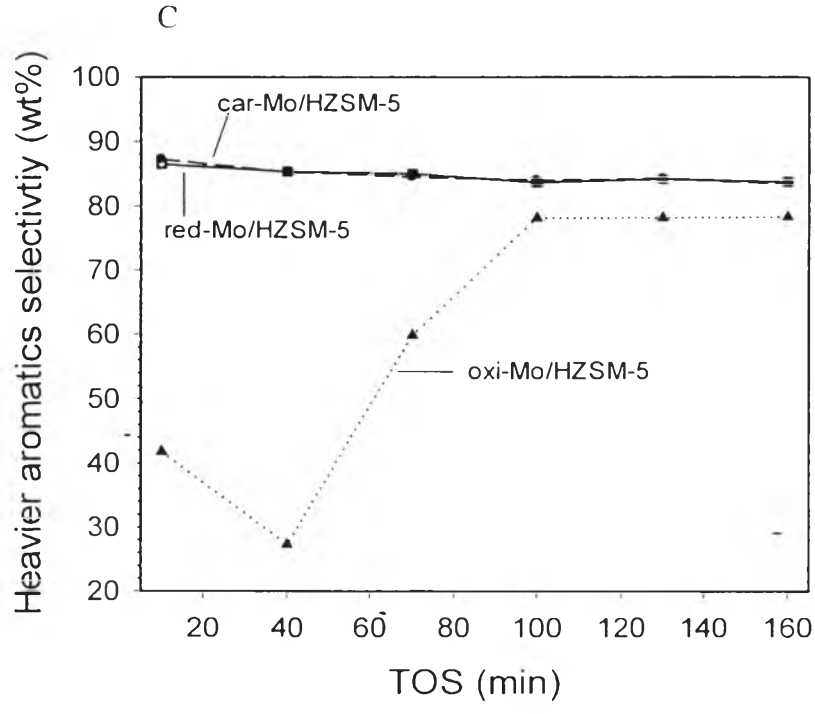

Figure 6.5 (A) Benzene conversions vs. TOS of red-Mo/ZSM-5 (solid line), oxi-Mo/ZSM-5 (dotted line), and car-Mo/HZSM-5 (dash line), (B) toluene selectivity vs. TOS, (C) heavier aromatics vs. TOS.

6.4.3 Investigation of Catalyst Deactivation

Spent catalysts (after TOS of 160 min) were brought to perform XPS for the purpose of comparison with freshly treated catalysts, so that changes in activity could be linked with Mo and/or C species. The resulting XPS spectra are shown in Figure 6.6 for Mo3d region and in Figure 6.7 for C1s region. Considering the most highly active red-Mo/HZSM-5 catalyst, it is clear that a decrease in activity is attributed to an oxidation of metallic Mo, as evidenced by a significant shift of $Mo3d_{5/2}$ peak to higher binding energy. Based on the XPS spectrum (a) at Mo3d region in Figure 6.6, at TOS of 160 min, Mo^{5+}/Mo^{6+} species dominate in the spent catalyst and cause the catalyst activity to decrease. Moreover, by the XPS result at the C1s region in Figure 6.7, the spent catalyst possibly contains Mo_2C and MoO_xC_y species, which is implied from the peaks of Mo_2C and carbidic carbon, respectively. Together with a small peak of $Mo3d_{5/2}$ at 227.9 eV appearing in spectrum (a) in

Figure 6.6, formation of Mo_2C can be declared. These two Mo carbide species are possibly generated during the reaction, in agreement with previous reports (Bouchy et al., 2000; Derouane-Abd Hamid et al., 2000; Liu et al., 2006), and play some role in catalyst activity, as benzene conversion is shown in Figure 6.5(A). Coke formation in forms of graphitic/amorphous carbon and polymeric carbon is also a cause of catalyst deactivation. It has been reported that carbon species can be distinguished by the C1s binding energy, for example carbidic carbon (283.3 eV), polymeric carbon (284.5 eV), and amorphous or graphitic carbon (285.0 eV) (Leclercq et al., 1989; Ledoux et al., 1992). In the case of oxi-Mo/HZSM-5, changes in activity can be described by changes in the nature of the Mo species. At TOS of 160 min where this catalyst showed the highest activity compared with the other two, the presence of Mo species is also in agreement. Mo^{5+} dominates in this spent catalyst as shown in Figure 6.6 and plays a role in activity more significant than the mixture of Mo^{5+} and Mo^{6+}. Compared with the spectrum of the fresh catalyst, a significant shift of the $Mo3d_{5/2}$ peak to lower binding energy suggests the reduction of Mo^{6+} (MoO_3), possibly by CH_4 and/or H_2 by products, during the reaction. There is a possibility of a changing progression of Mo species, namely Mo^{6+} changed into Mo^0 at around TOS of 90 min and provided the best catalyst activity, and after that it tended to oxidize and convert into Mo^{5+} species at TOS of 160 min, as indicated by the XPS spectrum. In addition to Mo^{5+} species, MoO_xC_y species were also likely formed according to the peak of carbidic carbon at 283.3 eV in spectrum (b) of Figure 6.7. This may also help promote the reaction. For car-Mo/HZSM-5, a shift of $Mo3d_{5/2}$ peak to higher binding energy suggested an oxidation of Mo species, especially Mo^{5+} and Mo^0 species. Referring to the XPS spectrum, spent car-Mo/HZSM-5 mainly consists of Mo^{6+} species with some Mo^{4+} species. The $Mo3d_{5/2}$ binding energies were 233.1 eV for Mo^{6+}, 231.4 eV for Mo^{5+}, 229.8 eV for Mo^{4+}, 227.6 eV for Mo^0/Mo_2C (Solymosi et al., 1995; Wang et al., 1997). Losses of $Mo3d_{5/2}$ peak at 227.9 eV and C1s peak at 283.9 eV of spent car-Mo/HZSM-5 suggest losses of Mo_2C species during the reaction. A shift of C1s peak to higher binding energy indicates graphitic/amorphous carbon formation (B.E. = 285.0 eV). Hence, a slight decrease in catalyst activity of this catalyst is not only due to an oxidation of Mo species, but also due to coke covered on catalyst surface.

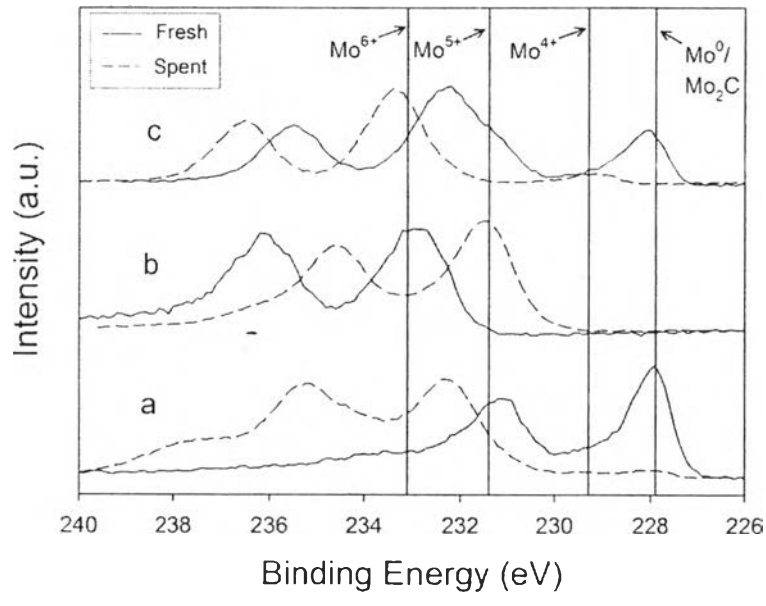

Figure 6.6 A comparative XPS spectra at Mo3d region between (solid line) fresh and (dashed line) spent (at TOS of 160 min) Mo/HZSM-5 catalyst, including (a) red-Mo/HZSM-5, (b) oxi-Mo/HZSM-5, and (c) car-Mo/HZSM-5.

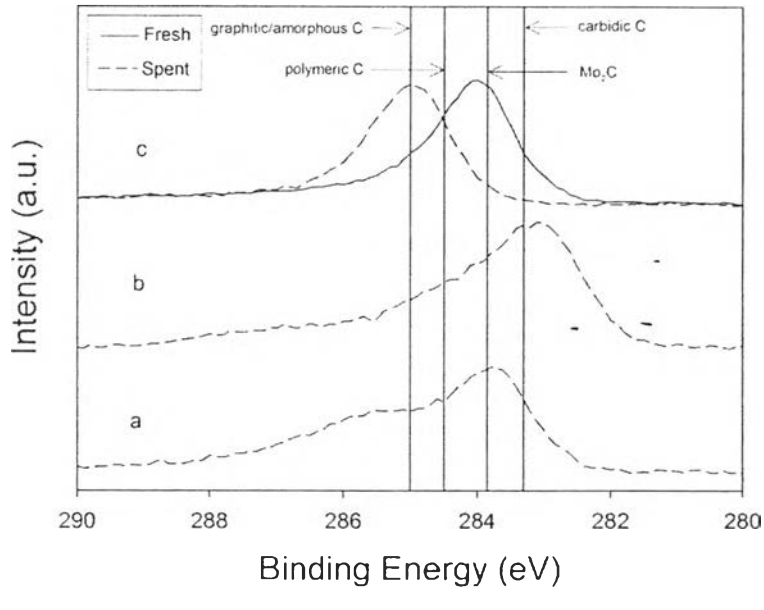

Figure 6.7 A comparative XPS spectra at C1s region between (solid line) fresh and (dashed line) spent (at TOS of 160 min) Mo/HZSM-5 catalyst, including (a) red-Mo/HZSM-5, (b) oxi-Mo/HZSM-5, and (c) car-Mo/HZSM-5.

6.4.4 Effect of H_2 Co-feed

It was known from the previous part that metallic Mo is the most reactive species of Mo for the reaction; however, metallic Mo is susceptible to the reaction conditions, as it tends to oxidize during the reaction. Moreover, though the catalyst is active, heavier aromatics are largely generated, especially naphthalene Thus, to maintain Mo in the metallic form and to depress the formation of heavier aromatics with increasing toluene selectivity, the addition of H_2 co-feed was proposed and H_2 content was also varied. The strategy of this testing was based on *Le Chatelier's* principle that the benzene coupling reaction could be pushed backwards to the left-hand-side by H_2. As expected, adding H_2 minimized naphthalene formation and other heavier aromatics with enhancing toluene selectivity as shown in Figure 6.8. However, benzene conversion dropped significantly after adding 37.50% H_2 and slightly decreased with increasing amount of H_2. On the other hand, toluene selectivity appears to be rather stable at around 80 wt% after adding 37.50 % H_2. As naphthalene formation was suppressed by H_2 addition, the methylation reaction of benzene into toluene became a major reaction; however, this reaction proceeds rather slowly. For the effect of H_2 co-feed on retarding oxidation of metallic Mo, it was revealed by the XPS results in Figure 6.9 that adding H_2 doesn't help prevent the oxidation of metallic Mo, even adding H_2 up to 75% in feed. Like spent catalyst run without H_2, the spent catalysts run with 50% or 75% H_2 contain Mo^{6+} and Mo^{5+} species, as clearly shown in Figure 6.9. A small fraction of Mo_2C likely existed as the XPS results at C1s region testify in Figure 6.10. In addition, adding H_2 seems to prevent coke formation on the catalyst surface.

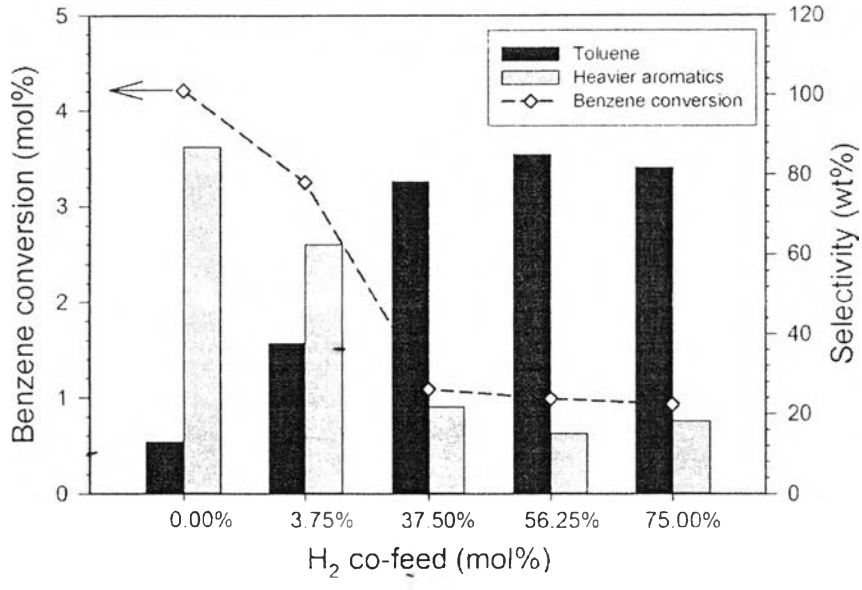

Figure 6.8 Benzene conversion and product selectivity at TOS of 40 min as a function of percentage of H_2 co-feed. Reaction conditions: red-Mo/HZSM-5(Mo/Al = 0.5), T = 550 °C, M/B ratio = 70, WHSV = 3.7 h^{-1}.

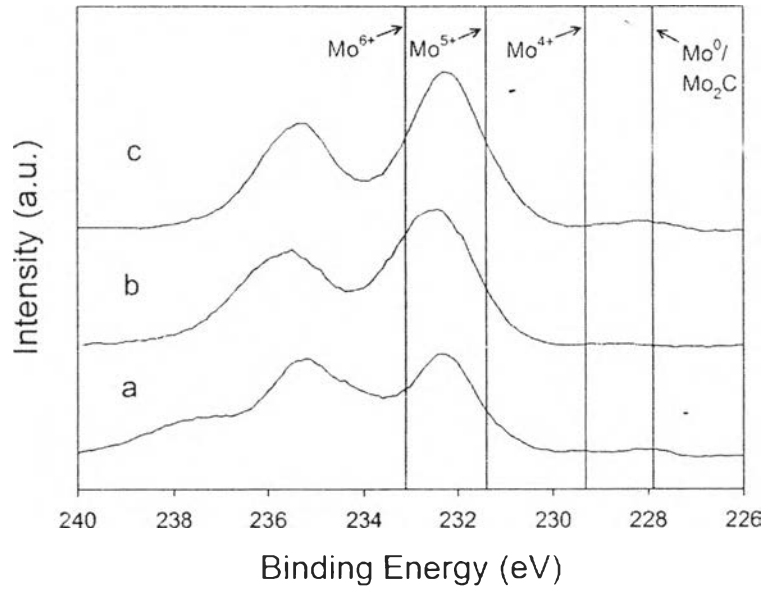

Figure 6.9 XPS spectra of spent Mo/HZSM-5 catalysts at Mo3d region, including (a) red-Mo/HZSM-5 without H_2 co-feed, (b) red-Mo/HZSM-5 with 50% H_2 co-feed, (c) red-Mo/HZSM-5 with 75% H_2 co-feed.

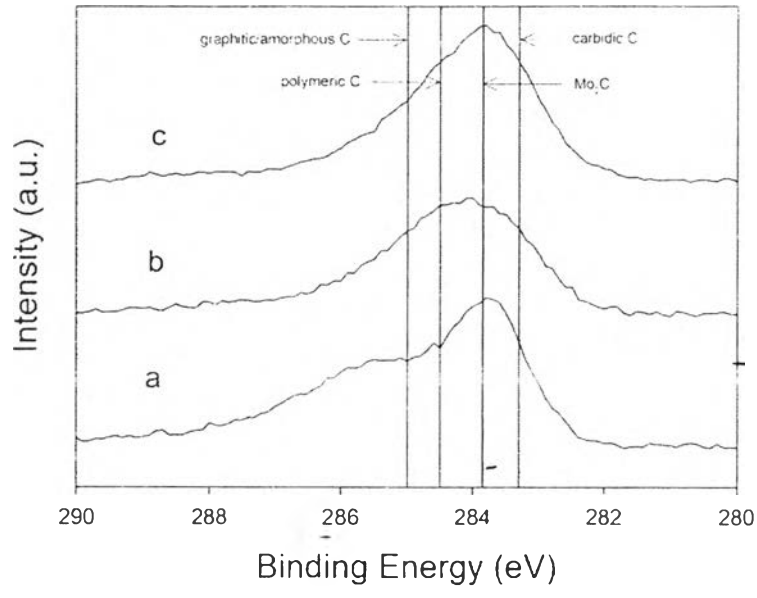

Figure 6.10 XPS spectra of spent Mo/HZSM-5 catalysts at C1s region, including (a) red-Mo/HZSM-5 without H_2 co-feed, (b) red-Mo/HZSM-5 with 50%H_2 co-feed, (c) red-Mo/HZSM-5 with 75%H_2 co-feed.

6.4.5 Effect of Reaction Temperature

Results of the effect of reaction temperature on benzene conversion and on product selectivity are portrayed in Figure 6.11. Reaction temperature plays a significant role in both activity and product selectivity. No reaction occurred at 350 °C, while increasing temperature activates the reaction. Benzene conversion increases with increasing reaction temperature. This is because of the highly endothermic nature of this reaction. At low temperature (e.g., 400 °C and 450°C), the fraction of toluene is lower compared to its fraction at higher temperature. This might be because the temperature is not appropriate to activate the methylation reaction. Methylation of benzene into toluene is favored at higher temperature and especially at 500 °C and 550°C, where toluene selectivity is above 80%. Nevertheless, at too high of a temperature the reaction tends to contribute to more heavy aromatics formation, as evidenced by an increase in the heavier aromatic fraction with the reaction temperature from 500 °C to 700°C. Therefore, the most appropriate reaction temperature is at 550 °C, in which benzene conversion and toluene selectivity are compromised.

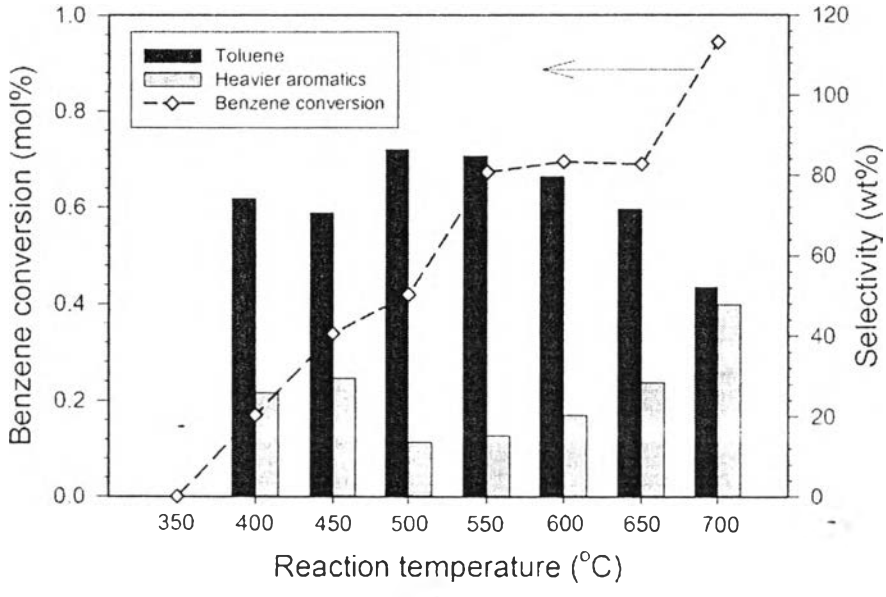

Figure 6.11 Benzene conversion and product selectivity at TOS of 40 min as a function of reaction temperature. Reaction conditions: red-Mo/HZSM-5(Mo/Al = 0.5), 75%H_2 co-feed, M/B ratio = 70, WHSV = 3.7 h^{-1}.

6.4.6 Effect of Mo Loading

Figure 6.12 shows the effect of Mo loading on benzene conversion and product selectivity. Increasing Mo increases benzene conversion while toluene selectivity slightly increases. This result stresses a role of Mo in activating the reaction as a result of improving benzene conversion. Studies on the acid strength of this catalyst using TPD-NH_3 revealed that adding more Mo decreases strong acid sites but increases weak acid sites, as illustrated in Figure 6.13. In the TPD-NH_3 profile, the first peak at lower temperature represents weak acid sites, while the peak at higher temperature is due to strong acid sites (Ouyang et al., 2013). This suggests the preference of Mo in being associated with strong acid sites. Product selectivity appears to be related to acid strength of the catalyst, namely a lessening in strong acid sites slightly decreases heavy aromatics formation with slight increases in toluene formation.

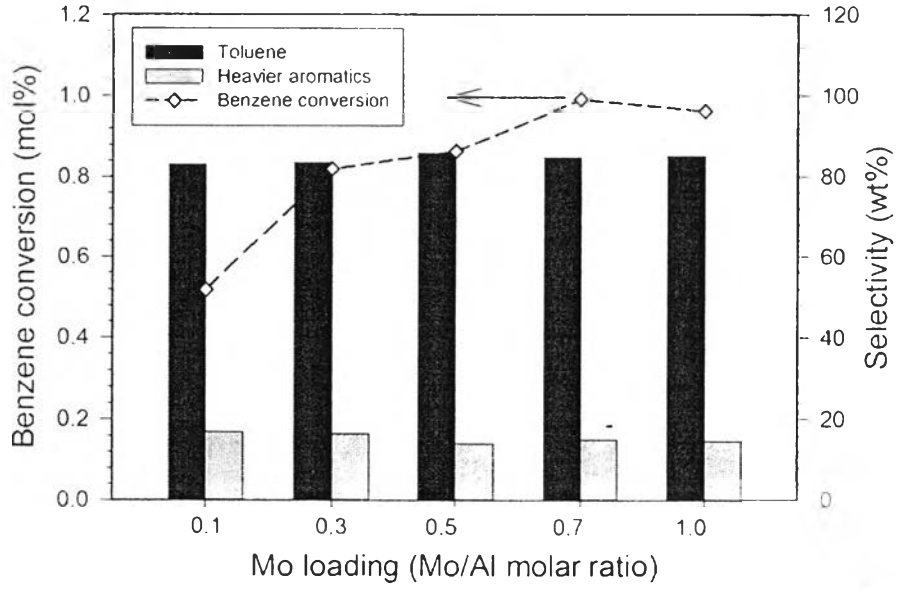

Figure 6.12 Benzene conversion and product selectivity at TOS of 40 min as a function of Mo loading. Reaction conditions: red-Mo/HZSM-5, T = 550 °C, 75%H_2 co-feed, M/B ratio = 70, WHSV = 3.7 h^{-1}.

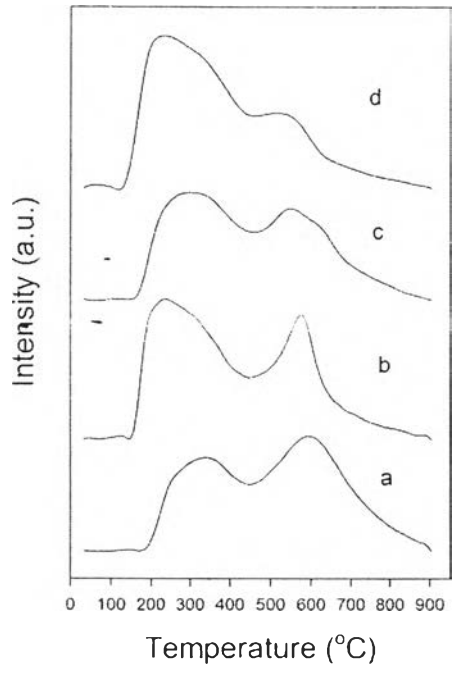

Figure 6.13 TPD-NH3 profiles of (a) HZSM-5, (b) Mo/HZSM-5 with Mo/Al : 0.1, (c) Mo/HZSM-5 with Mo/Al : 0.5, (d) Mo/HZSM-5 with Mo/Al : 1.0.

6.4.7 Effect of Methane to Benzene Feed Molar Ratio

Based on Le Chatelier's principle, increasing the concentration of reactant could force the reaction forwards. This principle holds true in this case only at methane/benzene molar ratio of 20 and 70 as shown a Figure 6.14. Benzene conversion increases from 0.6% to 0.95% when increase the ratio from 20 to 70, while selectivity remains unchanged. However, at a ratio higher than 70, benzene conversion decreases and it appears to decrease with increasing amount of methane. Interestingly, toluene selectivity was improved when increasing the methane/benzene molar ratio. A decrease in benzene conversion is likely attributed to a lower concentration of benzene, thus lowering the probability of benzene coupling. Once benzene coupling had been suppressed by adding more methane, benzene methylation became more significant, as toluene dominates in the reaction products particularly at the ratio of 142, in which toluene selectivity increases to 95%. Unfortunately, benzene conversion is still very low.

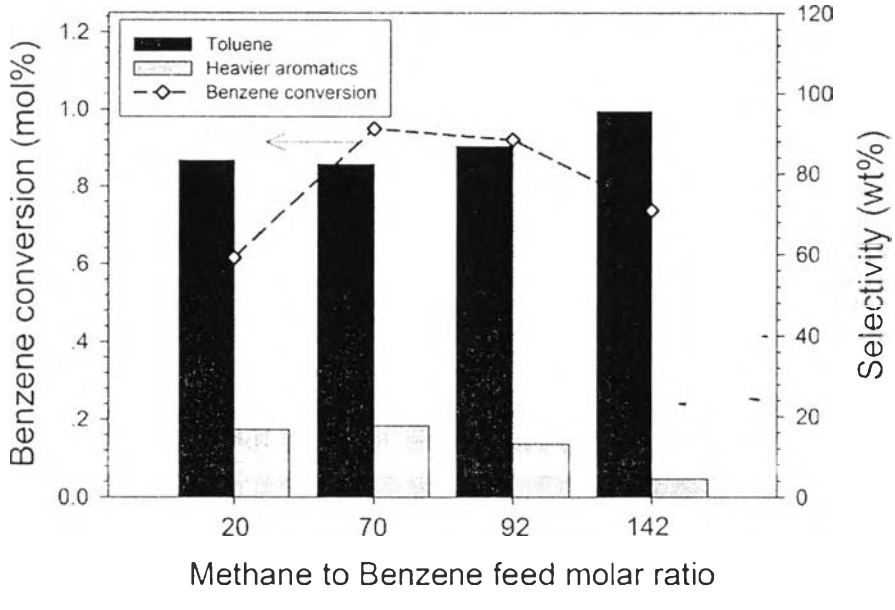

Figure 6.14 Benzene conversion and product selectivity at TOS of 40 min as a function of methane to benzene feed molar ratio. Reaction conditions: red-Mo/HZSM-5 (Mo/Al : 0.7), T = 550 °C, 75%H_2 co-feed, WHSV = 3.7 h^{-1}.

6.4.8 Effect of WHSV

Figure 6.15 illustrates the effect of space velocity (WHSV) on benzene conversion and product selectivity. As expected, benzene conversion increases with decreasing weight hourly space velocity (WHSV). At low WHSV, reactants have more time to contact with the catalyst and, subsequently, perform the reaction. On the other hand, less contact time at high WHSV results in lower benzene conversion; however, toluene selectivity was slightly improved. It is implied that the benzene coupling reaction may require greater retention time to complete the reaction, while methane activation may not require as much; the methylation reaction of benzene with activated methane species requires much more time.

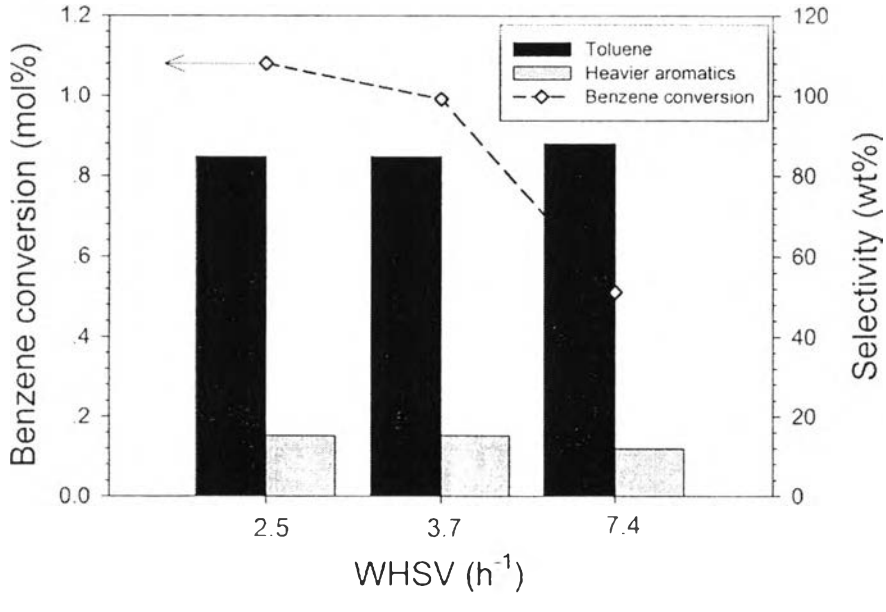

Figure 6.15 Benzene conversion and product selectivity at TOS of 40 min as a function of WHSV. Reaction conditions: red-Mo/HZSM-5 (Mo/Al : 0.7), T = 550 °C, 75%H_2 co-feed, M/B ratio = 70.

6.5 Conclusion

Mo/HZSM-5 can activate the methylation of benzene with methane, but this desired reaction significantly competes with the benzene coupling reaction, in which naphthalene is dominant. Metallic Mo is the most active form of Mo in HZSM-5 for the reaction, which can be obtained by reduction of Mo/HZSM-5 at high temperature under H_2 atmosphere. However, metallic Mo is susceptible to the reaction conditions as it tends to be oxidized during the reaction. In addition to metallic Mo, Mo_2C and MoO_xC_y species likely play a role for the reaction. Adding H_2 cannot prevent oxidation of metallic Mo during the reaction; however, it can suppress naphthalene, other heavy aromatics, and coke formation with enhancing toluene selectivity, but benzene conversion significantly dropped with increasing H_2. Reaction temperature has an influence on both benzene conversion and product selectivity. Mo/HZSM-5 with higher Mo loading increases benzene conversion but just slightly improves toluene selectivity. Moreover, methane to benzene feed molar ratio and space velocity affect both benzene conversion and product selectivity.

6.6 Acknowledgements

This work was financially supported by the Thailand Research Fund through the Royal Golden Jubilee Ph.D. Program (PHD/0177/2552) and by the PTT Global Chemical Public Company Limited. The use of the scientific instruments was supported by the Analytical and Testing Service Center of the Research Affairs of The Petroleum and Petrochemical College, Chulalongkorn University.

6.7 References

Adebajo, M., Long, M.A., and Howe, R.F. (2000) Methane activation over zeolite catalysts: the methylation of benzene. Research on Chemical Intermediates, 26(2), 185-191.

Barath, F., Turki, M., Keller, V., and Maire, G. (1999) Catalytic activity of reduced MoO_3/α-Al_2O_3 for hexanes reforming: I. preparation, characterization, and

X-ray photoelectron spectroscopy studies. Journal of Catalysis, 185(1), 1-11.

Barthos, R., Bánsági, T., Süli Zakar, T., and Solymosi, F. (2007) Aromatization of methanol and methylation of benzene over Mo_2C/ZSM-5 catalysts. Journal of Catalysis, 247(2), 368-378.

Bohne, Y., Shevchenko, N., Prokert, F., von Borany, J., Rauschenbach, B., and Möller, W. (2005) In situ characterization of phase formation during high-energy oxygen ion implantation in molybdenum. Nuclear Instruments and Methods in Physics Research Section B: Beam Interactions with Materials and Atoms, 240(1–2), 157-161.

Bouchy, C., Schmidt, I., Anderson, J.R., Jacobsen, C.J.H., Derouane, E.G., and Derouane-Abd Hamid, S.B. (2000) Metastable fcc α-$MoC_{(1-x)}$ supported on HZSM5: preparation and catalytic performance for the non-oxidative conversion of methane to aromatic compounds. Journal of Molecular Catalysis A: Chemical, 163(1-2), 283-296.

Chen, J.G. (1995) Selective activation of C-H and C-C bonds on metal carbides: A comparison of reactions of n-butane and 1,3-butadiene on vanadium carbide films on V(110). Journal of Catalysis, 154(1), 80-90.

Chen, L.Y., Lin, L.W., Xu, Z.S., Li, X.S., and Zhang, T. (1995) Dehydro-oligomerization of methane to ethylene and aromatics over molybdenum/HZSM-5 catalyst. Journal of Catalysis, 157(1), 190-200.

Derouane-Abd Hamid, S.B., Anderson, J.R., Schmidt, I., Bouchy, C., Jacobsen, C.J.H., and Derouane, E.G. (2000) Effect of the activation procedure on the performance of Mo/H-MFI catalysts for the non-oxidative conversion of methane to aromatics. Catalysis Today, 63(2-4), 461-469.

deVries, J.E., Yao, H.C., Baird, R.J., and Gandhi, H.S. (1983) Characterization of molybdenum-platinum catalysts supported on γ-alumina by X-ray photoelectron spectroscopy. Journal of Catalysis, 84(1), 8-14.

Jiang, H., Wang, L., Cui, W., and Xu, Y. (1999) Study on the induction period of methane aromatization over Mo/HZSM-5: partial reduction of Mo species and formation of carbonaceous deposit. Catalysis Letters, 57(3), 95-102.

Kennedy, E.M., Lonyi, F., Ballinger, T.H., Rosynek, M.P., and Lunsford, J.H. (1994) Conversion of benzene to substituted aromatic products over zeolite catalysts at elevated pressures. Energy & Fuels, 8(4), 846-850.

Leclercq, L., Provost, M., Pastor, H., Grimblot, J., Hardy, A.M., Gengembre, L., and Leclercq, G. (1989) Catalytic properties of transition metal carbides: I. preparation and physical characterization of bulk mixed carbides of molybdenum and tungsten. Journal of Catalysis, 117(2), 371-383.

Ledoux, M.J., Huu, C.P., Guille, J., and Dunlop, H. (1992) Compared activities of platinum and high specific surface area Mo_2C and WC catalysts for reforming reactions: I. catalyst activation and stabilization: reaction of n-hexane. Journal of Catalysis, 134(2), 383-398.

Lee, J.S., Oyama, S.T., and Boudart, M. (1987) Molybdenum carbide catalysts. I. synthesis of unsupported powders. Journal of Catalysis, 106(1), 125-133.

Liu, B., Yang, Y., and Sayari, A. (2001) Non-oxidative dehydroaromatization of methane over Ga-promoted Mo/HZSM-5-based catalysts. Applied Catalysis A: General, 214(1), 95-102.

Liu, H., Bao, X., and Xu, Y. (2006) Methane dehydroaromatization under nonoxidative conditions over Mo/HZSM-5 catalysts: identification and preparation of the Mo active species. Journal of Catalysis, 239(2), 441-450.

Lukyanov, D.B. and Vazhnova, T. (2009) Selective and stable benzene alkylation with methane into toluene over PtH-MFI bifunctional catalyst. Journal of Molecular Catalysis A: Chemical, 305(1–2), 95-99.

Ma, D., Shu, Y., Bao, X., and Xu, Y. (2000) Methane dehydro-aromatization under nonoxidative conditions over Mo/HZSM-5 catalysts: EPR study of the Mo species on/in the HZSM-5 zeolite. Journal of Catalysis, 189(2), 314-325.

Mcketta, J.J. (1993). Chemical Processing Handbook, New York: Marcel Dekker.

Ouyang, Q., Yin, S.-F., Chen, L., Zhou, X.-P., and Au, C.-T. (2013) A new catalytic process for high-efficiency synthesis of p-xylene by methylation of toluene with CH_3Br. AIChE Journal, 59(2), 532-540.

Regalbuto, J. and Ha, J.W. (1994) A corrected procedure and consistent interpretation for temperature programmed reduction of supported MoO_3. Catalysis Letters, 29(1-2), 189-207.

Solymosi, F., Cserényi, J., Szöke, A., Bánsági, T., and Oszkó, A. (1997) aromatization of methane over supported and unsupported Mo-based catalysts. Journal of Catalysis, 165(2), 150-161.

Solymosi, F., Erdöhelyi, A., and Szöke, A. (1995) Dehydrogenation of methane on supported molybdenum oxides. formation of benzene from methane. Catalysis Letters, 32(1-2), 43-53.

Solymosi, F., Szöke, A., and Cserényi, J. (1996) Conversion of methane to benzene over Mo_2C and Mo_2C/ZSM-5 catalysts. Catalysis Letters, 39(3-4), 157-161.

Szöke, A. and Solymosi, F. (1996) Selective oxidation of methane to benzene over K_2MoO_4/ZSM-5 catalysts. Applied Catalysis A: General, 142(2), 361-374.

Wang, D., Lunsford, J.H., and Rosynek, M.P. (1997) Characterization of a Mo/ZSM-5 catalyst for the conversion of methane to benzene. Journal of Catalysis, 169(1), 347-358.

Wang, L. and Tysoe, W.T. (1991) An investigation of ethylene hydrogenation catalyzed by metallic molybdenum using an isolatable high-pressure reactor: identification of the reaction site and the role of carbonaceous deposits. Journal of Catalysis, 128(2), 320-336.

Weckhuysen, B., Rosynek, M., and Lunsford, J. (1998) Characterization of surface carbon formed during the conversion of methane to benzene over Mo/H-ZSM-5 catalysts. Catalysis Letters, 52(1-2), 31-36.

Williams, C.C., Ekerdt, J.G., Jehng, J.M., Hardcastle, F.D., and Wachs, I.E. (1991) A Raman and ultraviolet diffuse reflectance spectroscopic investigation of alumina-supported molybdenum oxide. The Journal of Physical Chemistry, 95(22), 8791-8797.

Zhang, C.L., Li, S., Yuan, Y., Zhang, W.-X., Wu, T.H., and Lin, L.W. (1998) Aromatization of methane in the absence of oxygen over Mo-based catalysts supported on different types of zeolites. Catalysis Letters, 56(4), 207-213.